CCY032	a his3-Δ1 leu2-Δ1 ura3-Δ0 met15-Δ1 RAX2-GFP-kanMX6::RAX2	see text
CCY033	α his3-Δ1 leu2-Δ1 ura3-Δ0 lys-Δ0 RAX2-GFPkanMX6::RAX2	see text
CCY034	a/α his3-Δ1/his3-Δ1 leu2-Δ1/leu2-Δ1 ura3-Δ0/ura3-Δ0 met15-Δ1/lys-Δ0 RAX2-GFP-kanMX6::RAX2/RAX2-GFP-kanMX6::RAX2	mating of CCY032 and CCY033
CCY035	a his3-Δ1 leu2-Δ1 ura3-Δ0 met15-Δ1 RAX2-GFP-kanMX6::RAX2 bud32 Δ::kanMX6	segregant from CCY002xCCY032
CCY036	a/α his3-Δ1/his3-Δ1 leu2-Δ1/leu2-Δ1 ura3-Δ0/ura3-Δ0 met15-Δ1/met15-Δ1 RAX2-GFP-kanMX6::RAX2/RAX2-GFP-kanMX6::RAX2bud32 Δ::kanMX6/bud32 Δ::kanMX6	a/α conversion from CCY035
CCY037	a his3-Δ1 leu2-Δ1 ura3-Δ0 met15-Δ1 RAX2-GFP-kanMX6::RAX2 cgi121 Δ::kanMX6	segregant from CCY005xCCY032
CCY038	a/α his3-Δ1/his3-Δ1 leu2-Δ1/leu2-Δ1 ura3-Δ0/ura3-Δ0 met15-Δ1/met15-Δ1 RAX2-GFP-kanMX6::RAX2/RAX2-GFP-kanMX6::RAX2 cgi121 Δ::kanMX6/cgi121 Δ::kanMX6	a/α conversion from CCY037
CCY039	a/α his3-Δ1/his3-Δ1 leu2-Δ1/leu2-Δ1 ura3-Δ0/ura3-Δ0 met15-Δ1/lys-Δ0 RAX2-GFP-kanMX6::RAX2/RAX2-GFP-kanMX6::RAX2 gon7 Δ::hisMX6/GON7	see text
CCY040	a his3-Δ1 leu2-Δ1 ura3-Δ0 met15-Δ1 RAX2-GFP-kanMX6::RAX2 gon7 Δ::hisMX6	segregant from CCY039
CCY041	a/α his3-Δ1/his3-Δ1 leu2-Δ1/leu2-Δ1 ura3-Δ0/ura3-Δ0 met15-Δ1/met1 RAX2-GFP-kanMX6::RAX2/ RAX2-GFP-kanMX6::RAX2 gon7 Δ::hisMX6/gon7 Δ::hisMX6	a/α conversion from CCY040
CCY042	a his3-Δ1 leu2-Δ1 ura3-Δ0 met15-Δ1 rax2 Δ::kanMX6	EUROSCARF
CCY043	α his3-Δ1 leu2-Δ1 ura3-Δ0 lys-Δ0 rax2 Δ::kanMX6	Open Biosystems, Inc.
CCY044	a/α his3-Δ1/his3-Δ1 leu2-Δ1/leu2-Δ1 ura3-Δ0/ura3-Δ0 met15-Δ1/lys-Δ0 rax2 Δ::kanMX6/rax2 Δ::kanMX6	mating of CCY042 and CCY043
CCY045	α his3-Δ1 leu2-Δ1 ura3-Δ0 lys-Δ0 rax2 Δ::kanMX6 bud32 Δ::kanMX6	segregant from CCY002xCCY042
CCY046	a/α his3-Δ1/his3-Δ1 leu2-Δ1/leu2-Δ1 ura3-Δ0/ura3-Δ0 lys-Δ0/lys-Δ0 rax2 Δ::kanMX6/rax2 Δ::kanMX6 bud32 Δ::kanMX6/bud32 Δ::kanMX6	a/α conversion from CCY045
CCY047	α his3-Δ1 leu2-Δ1 ura3-Δ0 lys-Δ0 rax2 Δ::kanMX6 cgi121 Δ::kanMX6	segregant from CCY005xCCY042
CCY048	a/α his3-Δ1/his3-Δ1 leu2–Δ1/leu2-Δ1 ura3-Δ0/ura3-Δ0 lys-Δ0/lys-Δ0 rax2 Δ::kanMX6/rax2 Δ::kanMX6 cgi121 Δ::kanMX6/cgi121 Δ::kanMX6	a/α conversion from CCY047

CCY049	a/ α his3-Δ1/his3-Δ1 leu2-Δ1/leu2-Δ1 ura3-Δ0/ura3-Δ0 met15-Δ1/met15-Δ1 rax2Δ::kanMX6/rax2Δ::kanMX6 gon7Δ::hisMX6/GON7	see text
CCY050	a his3-Δ1 leu2-Δ1 ura3-Δ0 met15-Δ1 rax2Δ::kanMX6 gon7Δ::hisMX6	segregant from CCY049
CCY051	a/ α his3-Δ1/his3-Δ1 leu2-Δ1/leu2-Δ1 ura3-Δ0/ura3-Δ0 met15-Δ1/met15-Δ1 rax2Δ::kanMX6/rax2Δ::kanMX6 gon7Δ::hisMX6/gon7Δ::hisMX6	a/ α conversion from CCY050
CCY052	a his3-Δ1 leu2-Δ1 ura3-Δ0 met15-Δ1 BUD32-GFP::BUD32	see text
CCY053	a/ α his3-Δ1/his3-Δ1 leu2-Δ1/leu2-Δ1 ura3-Δ0/ura3-Δ0 met15-Δ1/met15-Δ1 BUD32-GFP::BUD32/BUD32-GFP::BUD32	a/ α conversion from CCY052
CCY054	a his3-Δ1 leu2-Δ1 ura3-Δ0 met15-Δ1 BUD32(K52A)-GFP::BUD32	see text
CCY055	α his3-Δ1 leu2-Δ1 ura3-Δ0 lys-Δ0 BUD32(K52A)-GFP::BUD32	see text
CCY056	a/ α his3-Δ1/his3-Δ1 leu2-Δ1/leu2-Δ1 ura3-Δ0/ura3-Δ0 met15-Δ1/ lys-Δ0 BUD32(K52A)-GFP::BUD32/BUD32(K52A)-GFP::BUD32	mating of CCY054 and CCY055
CCY057	a his3-Δ1 leu2-Δ1 ura3-Δ0 met15-Δ1 BUD32(K52A)-GFP::BUD32 bud8Δ::kanMX6	segregant from CCY10xCCY055
CCY058	a/ α his3-Δ1/his3-Δ1 leu2-Δ1/leu2-Δ1 ura3-Δ0/ura3-Δ0 met15-Δ1/met15-Δ1 BUD32(K52A)-GFP::BUD32/ BUD32(K52A)-GFP::BUD32 bud8Δ::kanMX6/ bud8Δ::kanMX6	a/ α conversion from CCY057
CCY059	a his3-Δ1 leu2-Δ1 ura3-Δ0 met15-Δ1 BUD32(K52A)-GFP::BUD32 bud9Δ::kanMX6	segregant from CCY12xCCY055
CCY060	a/ α his3-Δ1/his3-Δ1 leu2-Δ1/leu2-Δ1 ura3-Δ0/ura3-Δ0 met15-Δ1/met15-Δ1 BUD32(K52A)-GFP::BUD32/ BUD32(K52A)-GFP::BUD32 bud9Δ::kanMX6/ bud9Δ::kanMX6	a/ α conversion from CCY059
CCY062	a his3-Δ1 leu2-Δ1 ura3-Δ0 met15-Δ1 BUD32-13myc:BUD32	see text
CCY063	a/ α his3-Δ1/his3-Δ1 leu2-Δ1/leu2-Δ1 ura3-Δ0/ura3-Δ0 met15-Δ1/met15-Δ1 BUD32-13myc:BUD32/ BUD32-13myc:BUD32	a/ α conversion from CCY062
CCY064	a his3-Δ1 leu2-Δ1 ura3-Δ0 met15-Δ1 BUD32(K52A):BUD32	see text
CCY065	a his3-Δ1 leu2-Δ1 ura3-Δ0 met15-Δ1 BUD32(K52A)-13myc:BUD32(K52A)	see text
CCY066	a/ α his3-Δ1/his3-Δ1 leu2-Δ1/leu2-Δ1 ura3-Δ0/ura3-Δ0 met15-Δ1/met15-Δ1 BUD32(K52A)-13myc:BUD32(K52A)/ BUD32(K52A)-13myc:BUD32(K52A)	a/ α conversion from CCY065

CCY067	a his3-Δ1 leu2-Δ1 ura3-Δ0 met15-Δ1 BUD32 (S258A)-GFP::BUD32	see text
CCY068	a/α his3-Δ1/his3-Δ1 leu2-Δ1/leu2-Δ1 ura3-Δ0/ura3-Δ0 met15-Δ1/met15-Δ1 BUD32(S258A)-GFP:BUD32/BUD32(S258A)-GFP::BUD32	a/α conversion from CCY067
CCY069	a his3-Δ1 leu2-Δ1 ura3-Δ0 met15-Δ1 sch9Δ::kanMX6	Open Biosystems, Inc.
CCY070	a/α his3-Δ1/his3-Δ1 leu2-Δ1/leu2-Δ1 ura3-Δ0/ura3-Δ0 met15-Δ1/met15-Δ1 sch9Δ::kanMX6/sch9Δ::kanMX6	a/α conversion from CCY069
CCY071	a his3-Δ1 leu2-Δ1 ura3-Δ0 met15-Δ1 CDC11-GFP-kanMX6::CDC11	see text
CCY072	α his3-Δ1 leu2-Δ1 ura3-Δ0 lys-Δ0 CDC11-GFP-kanMX6::CDC11	see text
CCY073	a/α his3-Δ1/his3-Δ1 leu2-Δ1/leu2-Δ1 ura3-Δ0/ura3-Δ0 met15-Δ1/lys-Δ0 CDC11-GFP-kanMX6::CDC11/CDC11-GFP-kanMX6::CDC11	mating of CCY071 and CCY072
CCY074	a his3-Δ1 leu2-Δ1 ura3-Δ0 met15-Δ1 CDC11-GFP-kanMX6::CDC11 cgi121Δ::kanMX6/cgi121Δ::kanMX	segregant of CCY071xCCY005
CCY075	a/α his3-Δ1/his3-Δ1 leu2-Δ1/leu2-Δ1 ura3-Δ0/ura3-Δ0 met15-Δ1/met15-Δ1 CDC11-GFP-kanMX6::CDC11/CDC11-GFP-kanMX6::CDC11 cgi121Δ::kanMX6/cgi121Δ::kanMX6	a/α conversion from CCY074

440

a All strains are congenic to BY4743.

b The strain was generated by a precise replacement of the GON7 open reading frame by URA3.

Table S2 Plasmids used in this study

Plasmid	Description	Source
pBluescript (SK-)	Ampicillin (cloning)	Stratagene
pFA6a-kanMX	Kanamycin (integrative)	Longtine *et al.* (1998)
pFA6a-GFP^{S65T}-kanMX	Kanamycin (integrative)	Longtine *et al.* (1998)
pFA6a-13Myc-kanMX	Kanamycin (integrative)	Longtine *et al.* (1998)
pRS306	*URA3* (integrative)	Sikorski and Hieter (1989)
pRS425	*LEU2* (high copy)	Christianson *et al.* (1992)
pRS426	*URA3* (high copy)	Christianson *et al.* (1992)
pTM55	*Xho*I/*Sal*I fragment containing triple FLAG tag	our stock
pYC01	3138 bps *Xho*I/*Spe*I fragment containing *BUD8* gene in pRS425	see text
pYC02	3245 bps *Xho*I/*Spe*I fragment containing *BUD9* gene in pRS426	see text
pYC03	*Mlu*I restriction site at just downstream of start codon on *BUD8* in pYC01	see text
pYC04	*Mlu*I restriction site at just downstream of start codon on *BUD9* in pYC02	see text
pYC05	*Mlu*I fragments containing *GFP* sequence in pBluescript (SK-)	see text
pYC06	*GFP-BUD9* in pRS426	Kato *et al.* (2009)
pYC07	1460 bps fragment containing *GON7* gene in pBluescript (SK-)	see text
pYC08	1089 bps fragment without *GON7* gene in pBluescript (SK-)	see text
pYC09	*GON7*:: *URA3* in pBluescript (SK-)	see text
pYC10	*FLAG$_6$-BUD9* in pRS426	see text
pYC11	2094 bps *Spe*I/*Xho*I fragment containing *BUD32* in pBluescript (SK-)	see text
pYC12	*Mlu*I restriction site at just upstream of stop codon on *BUD32* in pYC11	see text
pYC13	*BUD32 (K52A)* in pBluescript (SK-)	see text
pYC14	*GFP-BUD8* in pRS425	Kato *et al.* (2009)
pYC15	*BUD32 (S258A)* in pBluescript (SK-)	see text
pYC16	*BUD32 (K52A)* in pRS306	see text
pYC17	*BUD32-GFP* in pBluescript (SK-)	see text
pYC18	*BUD32 (K52A)-GFP* in pBluescript (SK-)	see text
pYC19	*BUD32 (S258A)-GFP* in pBluescript (SK-)	see text
pYC20	*BUD32-GFP* in pRS306	see text

pYC21	*BUD32 (K52A)-GFP* in pRS306	see text
pCY22	*BUD32 (S258A)-GFP* in pRS306	see text

[a]The GFP sequences encode *GFP* with the S65T substitution.

442

Table S3 **Primers used in this study**

Primer	sequences
T7 promoter	TAATACGACTCACTATAGGG
M13 reverse	CAGGAAACAGCTATGAC
BUD8a	AAAAAA***CTCGAG***ACTTCAACCACCTTCA
BUD8b	AAAAAA***ACTAGT***AGAAGTACGGTTACAAGACT
BUD8c	***ACGCGT***ATACAATCAGACGAAG
BUD8d	CATACTTCATGTAGAATCG
BUD9a	AAAAAA***CTCGAG***CACAAGAACATTTCTG
BUD9b	AAAAAA***ACTAGT***CTCTATCGTACTCCTC
BUD9c	***ACGCGT***ACGAAAATAACCAGAG
BUD9d	CATTTCATAGGATGAAGAATG
BUD32a	AAAAAAACTAGTAAACGTCGATTTTACCAG
BUD32b	AAAAAACTCGAGGATAGTCATTCTTTCC
BUD32c	AAGAGAAGTATGCTAGGAACGCGTTAATATAAATGCTAGCG
BUD32d	GAGAAGTATGCTAGGAACGCGTTATAAATGCTAGCGTA
BUD32e	GCATATAGGCCACCAAAGCGTTATAG
BUD32f	GATAATATACTTTTGATGAGAATCCTTTGC
BUD32g	GCTATGCTAGGATAATATAAATGCTAGCG
BUD32h	TCTCTTACGACCACGCAACCTG
BUD32i	AAAAGATTCGAAGAGGTCAGGTTGCGTGGTCGTAAGAAGTATGCTAGGAGCAGGTCGA
BUD32j	TGTGCAGCGATATACAGGCAGTACGCTAGCATTTATATTAGAATTCGAGCTCGTTTAAAC
GFPa	AAAAAAACGCGTGGGTTAATTAACAGTAAA
GFPb	A***ACGCGT***TTTGTATAGTTCATCCATGCC
GFPc	A***GATATC***GGGTTAATTAACAGTAAAGGAG
GFPd	A***GATATC***TTTGTATAGTTCATCCATGCCATG
GON7a	AAAACTAGTAAATAGCGATTCTTCATCGTGAATG
GON7b	AAACTCGAGTAACGGTCATTTGTTTTAACACAG
GON7c	GCAACGATATGTAGCGCTAGAG
GON7d	***ACGCGT***TGAGATATTAGGATAAGGTTC

GON7e	TATACAGCCGATAGTGCACTGGAACCTTATCCTAATATCTCACGGATCCCCGGTTAATT
GON7f	GACTCTTTTCTGTTTGTATATACACTCTCTAGCGCTACATATCGT
URA3a	AAAA***ACGCGT***AAGCTTTGGCACATCAATG
URA3b	AAAA***ACGCGT***ACCGTTGTTATCAGAAATTC
RAX2a	AGAATGAAATGCTTGATACCGTCCCACCCGAAAAACTTATGAAGTTTGTCCGGATCCCCGGGTTAATTAA
RAX2b	AGTGTTCATTATTTTAAGTAGTTATATATTATATAATACAACCCCGATTAGAATTCGAGCTCGTTTAAAC
CDC11a	ATTGAAGCCAGGTTGGAAAAAGAGGCGAAAATCAAACAGGAAGAACGGATCCCCGGGTTAATTAA
CDC11b	ATATAGAGAAAGAAGAAATAAGTGAGGAAGCCAAAAGCGGACGAATTCGAGCTCGTTTAAAC

The bold italics indicate restriction sites.

Fragments of Genomic DNA Released by Injured Cells Activate Innate Immunity and Suppress Endocrine Function in the Thyroid

Akira Kawashima, Kazunari Tanigawa, Takeshi Akama, Huhehasi Wu, Mariko Sue, Aya Yoshihara, Yuko Ishido, Kouji Kobiyama, Fumihiko Takeshita, Ken J. Ishii, Hisashi Hirano, Hiroaki Kimura, Takafumi Sakai, Norihisa Ishii, and Koichi Suzuki

Laboratory of Molecular Diagnostics (A.K., K.T., T.A., H.W., M.S., A.Y., Y.I., K.S.), Department of Mycobacteriology, Leprosy Research Center, National Institute of Infectious Diseases, Tokyo 189-0002, Japan; Department of Molecular Biodefense Research (K.K., F.T.), Yokohama City University Graduate School of Medicine, Yokohama 236-0004, Japan; Laboratory of Adjuvant Innovation (K.K., K.J.I.), Department of Fundamental Research, National Institute of Biomedical Innovation, Osaka 567-0085, Japan; International Graduate School of Arts and Sciences (H.H.), Yokohama City University, Yokohama 230-0045, Japan; Area of Regulatory Biology (A.K., T.S.), Division of Life Science, Graduate School of Science and Engineering, Saitama University, Saitama 338-8570, Japan; Division of Bioimaging Sciences (H.K.), Center for Molecular Medicine, Jichi Medical University, Shimotsuke 329-0498, Japan; and Leprosy Research Center (N.I.), National Institute of Infectious Diseases, Tokyo 189-0002, Japan

Activation of innate and acquired immune responses, which can be induced by infection, inflammation, or tissue injury, may impact the development of autoimmunity. Although stimulation of cells by double-stranded DNA (dsDNA) has been shown to activate immune responses, the role of self-genomic DNA fragments released in the context of sterile cellular injury is not well understood. Using cultured thyroid cells, we show that cell injury prompts the release of genomic DNA into the cytosol, which is associated with the production of type I interferons, inflammatory cytokines, and chemokines. Molecules necessary for antigen processing and presentation to lymphocytes are also induced in thyroid cells by injury. dsDNA strongly suppressed the expression of sodium/iodide symporter and radioiodine uptake. To identify molecules responsible for sensing cytosolic dsDNA, we directly identified the cellular proteins that bound a dsDNA Sepharose column by mass spectrometry. Our analysis identified histone H2B, which was previously demonstrated to be an essential factor that mediates the activation of innate immunity induced by dsDNA. Knockdown of histone H2B using specific small interfering RNA abolished cell injury-induced innate immune activation and increased sodium/iodide symporter expression. These results indicate that genomic DNA fragments released by cell injury are recognized by extrachromosomal histone H2B, which results in the activation of genes involved in both innate and acquired immune responses in thyroid cells and suppression of thyroid function. These results suggest that sterile thyroid injury, in the absence of infection, may be sufficient to trigger autoimmune reaction and to induce thyroid dysfunction. (***Endocrinology*** **152: 1702–1712, 2011)**

The thyroid gland is one of the major organs targeted for autoimmune attack, resulting in the development of Graves' disease or Hashimoto's thyroiditis. It is assumed that autoimmune thyroid disease develops due to a combination of genetic susceptibility and environmental factors (1). However, the precise etiology and factors that trigger autoimmunity remain largely unknown. It has recently been well established that strong antigen-specific immune activation, such as that seen in autoimmune diseases, requires the prior activation of innate immunity (2).

ISSN Print 0013-7227 ISSN Online 1945-7170
Printed in U.S.A.

doi: 10.1210/en.2010-1132 Received October 1, 2010. Accepted December 29, 2010.
First Published Online February 8, 2011

Abbreviations: DNase, Deoxyribonuclease; DPBS, Dulbecco's phosphate buffered saline; dsDNA, double-stranded DNA; ESI, electrospray ionization; HRP, horseradish peroxidase; IFN, interferon; IRF, interferon regulatory factor; MHC, major histocompatibility complex; MS/MS, tandem mass spectrometry; NIS, sodium/iodide symporter; RIG-I, retinoic acid inducible gene I; RP, reversed-phase chromatography; SCX, strong cation exchange chromatography; siRNA, small interfering RNA; ssDNA, single-stranded DNA; Tg, thyroglobulin; ZBP1, Z-DNA binding protein 1.

Infection and/or cell injury trigger local innate immune activation, and the role of bacterial or viral infection on thyroid autoimmunity has been discussed previously. Molecular mimicry, antigen expression/spillage, and modification of self-components have been thought to provide the antigen-specific signals necessary for the induction of autoimmunity rather than tolerance (2), as shown by the possible role of *Yersinia enterocolitica* to induce Graves' disease via molecular mimicry (3). Other reports have suggested that viral infection triggers the expression of cytokines and chemokines and major histocompatibility complex (MHC) class II within locally infected tissues, which may result in the presentation of self-antigens and the development of autoimmunity in the absence of molecular mimicry (4). However, it remains to be determined whether infection is actually responsible for triggering thyroid autoimmunity or whether it is just an innocent bystander (5). It has been shown that immune reactions were also induced in thyroid cells in cases of excessive iodine intake, painless thyroiditis, or subacute thyroiditis (6–8). Apoptosis or necrosis is also reported to relate to the development of autoimmune thyroid diseases (9). All of these situations may result in the release of autoantigens and activation of immune responses, which in turn may stimulate an autoimmune reaction.

It has been shown that intracellular molecules released from dying or dead cells trigger sterile inflammation and activate immune responses (10, 11). Among endogenous molecules released from necrotic cells, genomic DNA was shown to induce the maturation of dendritic cells and to function as an adjuvant both *in vivo* and *in vitro* (12). Moreover, undigested genomic DNA in deoxyribonuclease (DNase) II knockout mice induced interferon (IFN)-β and TNF-α and caused chronic polyarthritis (13). In a previous study using thyroid cells, we demonstrated that cell injury-induced MHC class II expression correlated with the release of genomic DNA (14). This evidence strongly suggests that genomic DNA released from injured or dying cells facilitates the induction of innate and acquired immune responses.

Recently, several proteins have been reported to play roles in the recognition of double-stranded DNA (dsDNA) that mediate innate immune activation. Those include Z-DNA binding protein 1 [ZBP1, also known as DNA-dependent activator of IFN-regulatory factors (DAI)] (15), retinoic acid inducible gene I (RIG-I) (16, 17), absent in melanoma 2 (AIM2) (18), and extrachromosomal histone H2B (19). These reports have revealed that there are multiple recognition systems for sensing cytosolic dsDNA and that such systems may be different among species and cell types. For example, ZBP1 physically interacts with dsDNA and activates downstream signaling molecules TANK binding kinase-1 (TBK1) and interferon regulatory factor (IRF)-3. However, such effects were observed in mouse L929 cells (15) but not reproduced in mouse embryonic fibroblasts (20). RIG-I was reported to bind directly to dsDNA (16), whereas other investigators have reported that the action is through an RNA intermediate generated by RNA polymerase III transcription to induce IFN-β (17, 21).

In this report, we show that thyroid cell injury results in the release of genomic DNA fragments into the cytosol, which activates genes involved in both innate and acquired immune responses and suppresses thyroid endocrine function. We additionally show that extrachromosomal histone H2B is the factor responsible in the thyroid for sensing cytosolic DNA and mediating its action.

Materials and Methods

Cell culture and reagents

FRTL-5 rat thyroid cells were grown in Coon's modified Ham's F-12 medium containing 5% heat-treated, mycoplasma-free bovine serum (Invitrogen, Carlsbad, CA) and a mixture of six hormones (6H) containing bovine TSH (1 mU/ml), insulin (10 μg/ml), hydrocortisone (0.36 ng/ml), transferrin (5 μg/ml), glycyl-L-histidyl-L-lysine acetate (2 ng/ml), and somatostatin (10 ng/ml) as described (14). These reagents were purchased from Sigma-Aldrich (St. Louis, MO).

Cell injury

FRTL-5 cells suspended in Dulbecco's phosphate buffered saline (DPBS) were pulsed with a Gene Pulser (Bio-Rad Laboratories, Hercules, CA) set at 0.5 kV and at capacitance of 0, 250, 500, 750, and 1000 μF or pulsed twice with a capacitance of 1000 μF. Cells were washed with the medium and then cultured in a 10-cm^2 dish. Alternatively, cell damage was induced by removing culture medium and incubating at 37 C in a humidified 5% CO_2 incubator for 30 min. Cells were then cultured in culture medium up to 48 h.

Isolation of cytosol DNA fractionations by sucrose density-gradient centrifugation

Cytosolic DNA was prepared by modifying a method to prepare nuclear proteins (14, 22). Cells were centrifuged for 1 min in a microcentrifuge, then suspended in 500 μl of 0.3 M sucrose, 2% Tween-40, 10 mM HEPES KOH (pH 7.9), 10 mM KCl, 1.5 mM $MgCl_2$, and 0.1 mM EDTA and homogenized with pipetting 50 times with a yellow tip. The homogenate was overlaid on 500 μl of 1.5 M sucrose, 10 mM HEPES KOH (pH 7.9), 10 mM KCl, 1.5 mM $MgCl_2$, and 0.1 mM EDTA and centrifuged at 13,200 rpm for 10 min. The upper layer (~400 μl) was transferred to another tube, and cytosolic DNA was purified by phenol/chloroform extraction and ethanol precipitation. RNA was removed by incubating in 300 μl of 300 mM NaCl, 10 mM Tris-HCl (pH 7.4), 5 mM EDTA (pH 7.5), 40 μg/ml RNaseA (TAKARA BIO, Otsu, Japan) at 37 C for 30 min. Solution was again purified with phenol/chloroform extraction and ethanol precipitation, and the

TABLE 1. PCR primer sequences

Gene name	Forward primer (5′–3′)	Reverse primer (5′–3′)	Length (bp)
IFN-β	ACATTGCGTTCCTGCTGTGC	GCTCTTCAAGCCTAAAGTAGTCGTG	404
TNF-α	TCTCATCAGTTCCATGGCC	TGACTTTCTCCTGGTATGAAATGG	302
IL-6	TTCCAGCCAGTTGCCTTCTTGG	GGCATAGCACACTAGGTTTGCC	623
RFX5	TCTTGAAGCGGTCCTTCAGT	AGCTCGGGCTTCTAGCTCTT	245
CIITA	AGTTTCCATCCGTGGAAGTG	GTGGCAGCTCCTTGTCTTTC	159
MHC class I	GATGTATGGCTGTGACGTGG	ACACGGCATGTGTAATTCTGC	492
MHC class II	AGCAAGCCAGTCACAGAAGG	GATTCGACTTGGAAGATGCC	546
CD40	TGTTGCACAGGAGGATGGTA	CAGCACAAGCCACAAGTCAT	375
CD54	AGCCTCAGGCCTAAGAGGAC	AGGGGTCCCAGAGAGGTCTA	496
CD80	TTACAGTTGCCAGCTGATGC	ATGTTGGGGGTAGGGAAGTC	450
CD86	GTTCCTGTGAAGAGGCAAGC	AGGTTTCGGGTATCCTTGCT	429
CCL2	TAGCATCCACGTGCTGTCTC	TGAGGTGGTTGTGGAAAAGA	358
CCL4	CTCTCTCCTCCTGCTTGTGG	CACAGATTTGCCTGCCTTTT	200
CCL5	CCTCACCGTCATCCTCGTTG	TTCTTGAACCCACTTCTTCTCTGG	229
CXCL9	CTCATGGGCATCATCTTCCT	TCAGCTTCTTCACCCTTGCT	232
CXCL10	TCCGCATGTTGAGATCATTGCC	TTTGCCATCTCACCTGGACTGC	541
CXCL11	CCCTGGCTATGATCATCTGG	CCAGGCACCTTTGTCCTTTA	201
β-Actin	AGCCATGTACGTAGCCATCC	TGTGGTGGTGAAGCTGTAGC	220
VEGF promoter	AATGCTAGCCAGGCTATGGACCCTGGTAA	AATCTCGAGCAAGCCTCTGCGCTTCTC	186

DNA concentration was quantified using a NanoVue spectrometer (GE Healthcare, Little Chalfont, UK).

Transfection of double-stranded or single-stranded nucleic acids

One microgram of each synthetic DNA or RNA was mixed with 3 μl of Fugene6 transfection reagent (Roche Diagnostics, Basel, Switzerland) and 100 μl of serum-free medium and then incubated for 45 min at room temperature. FRTL-5 cells grown in six-well plastic plates (Greiner Bio One, Kremsmünster, Austria) to about 50% confluency were washed, and 100 μg of premade transfection mixture was added with 1 ml of serum-free medium. Cells were incubated for 6 h at 37 C in a CO_2 incubator before medium was replaced with normal culture medium containing serum. Cells were further incubated until mRNA or protein was extracted. Synthetic polynucleotides, poly(deoxyadenosine), poly(deoxyadenosine-deoxythymidined), poly(adenosine), and poly(inosine-cytosine) were purchased from GE Healthcare.

Total RNA isolation, RT-PCR, and quantitative real-time PCR

Total RNA was isolated from FRTL-5 cells using RNeasy Mini kits (QIAGEN, Hilden, Germany) with minor modifications of the manufacturer's protocol as described (23). To remove genomic DNA, RNA samples were incubated with DNase I (TAKARA BIO) at 37 C for 30 min. RNA was then purified by phenol/chloroform extraction and ethanol precipitation. One microgram of total RNA was reverse transcribed into cDNA using a High-Capacity cDNA Reverse Transcription Kit (Applied Biosystems, Foster City, CA). Touchdown PCR was performed using TaKaRa Ex *Taq* Hot Start version (TAKARA BIO) under the following conditions: 5 min at 94 C; 20 cycles of 30 sec at 94 C, 30 sec at 65–55 C (decreased in steps of 0.5 C/cycle until a temperature of 55 C was reached), 30 sec at 72 C; and then an additional 10–20 cycles (depending on the primer) of 30 sec at 94 C, 30 sec at 55 C, 30 sec at 72 C, and 7 min at 72 C. The PCR were separated by agarose gel electrophoresis, and the DNA bands were visualized under UV light. The PCR primers are listed in Table 1.

Quantitative real-time PCR was performed using TaqMan Gene Expression Master Mix (Applied Biosystems) on the ABI 7000 Real-Time PCR System (Applied Biosystems). The primers for sodium/iodide symporter (NIS) (Rn00583900_m1), thyroglobulin (Tg) (Rn00578496_m1), and β-actin (4352931E) were from Applied Biosystems. PCR conditions were follows: 2 min at 50 C, 10 min at 95 C, and 40 cycles of 15 sec at 95 C and 1 min at 60 C. β-Actin was used as an endogenous reference to calculate the relative expression levels of target genes according to Applied Biosystems' instructions.

Plasmid construction, transient transfection of plasmid, and reporter gene assay

pGL3 rat IFN-β was constructed using the rat IFN-β promoter region −173 to −31 (relative to the translation initiation site), which was PCR amplified from rat genomic DNA using the following primers, 5′-AATACGCGTAATGACAGAGGAAAACTGAAAGG-3′ (forward) and 5′-AATAGATCTTGCACGATGAGGCAAAGG-3′ (reverse). The PCR product was introduced into the *Mlu*I-*Bgl*II site of the pGL3 basic luciferase reporter plasmid (Promega, Madison, WI). Plasmid DNA was purified with the EndoFree Plasmid Maxi Kit (QIAGEN). The DNA sequence was analyzed using an ABI PRISM 310 Genetic Analyzer and GeneScan Collection software (Applied Biosystems).

FRTL-5 cells (1×10^4) plated on poly-D-lysine-coated 24-well plates (Greiner Bio One) were transfected with 0.3 μg of pGL3 rIFN-β using Fugene6 (Roche Diagnostics). Cells were then stimulated with 0.3 μg/500 μl per well of dsDNA or dsRNA, and the IFN-β promoter assay was performed with Bright-Glo Luciferase assay systems (Promega) 12 h after transfection. Luciferase activity was measured by FLUOstar galaxy (BMG LABTECH JAPAN, Saitama, Japan), and the data were normalized to corresponding protein concentrations, which was determined using a Bio-Rad DC Protein Assay Kit (Bio-Rad).

Iodide uptake

Iodide uptake was measured as described previously (24). Briefly, the culture medium was aspirated from FRTL-5 cells grown in 24-well plates and washed with Hanks' balanced salt solution [137 mM NaCl, 5.4 mM KCl, 1.3 mM $CaCl_2$, 0.4 mM $MgSO_4$, 0.5 mM $MgCl_2$, 0.4 mM Na_2HPO_4, 0.44 mM KH_2PO_4, and 5.55 mM glucose with 10 mM HEPES buffer (pH7.3)]. Cells were incubated with 0.1 μCi carrier-free ^{125}I at 37 C for 40 min and then washed with ice-cold DPBS and lysed with ice-cold ethanol by placing them at −20 C for 20 min, at which point the radioactivity of the iodide taken up by the cell was measured.

Isolation of dsDNA-binding molecules and electrospray ionization (ESI)-tandem mass spectrometry (MS/MS) analysis

Cytosolic proteins from FRTL-5 cells were prepared as previously described (14). Briefly, 5×10^6 cells were washed with DPBS and then lysed in 50 mM HEPES, 150 mM NaCl, 5 mM EDTA, 0.1% Nonidet P-40, and 20% glycerol in the presence of protease inhibitor cocktail (Complete Mini; Roche Diagnostics). After dialysis against 20 mM Tris-HCl (pH 8.0), 50 mM NaCl, 1 mM EDTA, and 1 mM β-mercaptoethanol, 4 ml of protein samples was mixed with 1.5 ml of single-stranded DNA (ssDNA) Sepharose, which was prewashed and equilibrated with equilibration buffer [20 mM Tris-HCl (pH 8.0), 50 mM NaCl, 1 mM EDTA, 1 mM β-mercaptoethanol, 10% glycerol, and 100 μg/ml BSA] at 4 C for 8 h. Samples were then applied to a column and washed with 3 ml of equilibration buffer, and flow-through fractions were collected as ssDNA-unbound samples. The samples were then mixed with dsDNA Sepharose, which was pretreated as ssDNA Sepharose, at 4 C for 24 h and applied on a column, washed with 5 ml of equilibration buffer four times, eluted with elution buffer [20 mM Tris-HCl (pH 8.0), 1 M NaCl, 1 mM EDTA, and 1 mM β-mercaptoethanol], and then concentrated by Centricon columns (Millipore, Billerica, MA).

The sample was reduced in 20 mM ammonium bicarbonate buffer (pH 8.0) containing 5 mM dithiothreitol at 80 C for 20 min and alkylated using 10 mM iodoacetamide at 37 C for 30 min in the same buffer, and then 1:50 (wt/wt) trypsin was added and incubated at 37 C for 3 h. After incubation, the same amount of trypsin was added and further incubated at 37 C for 12 h. The digestion was stopped by adding formic acid to a final concentration of 0.1%. Digested peptides were fractionated by strong cation exchange chromatography (SCX) followed by reversed-phase chromatography (RP). An online nano liquid chromatography system (Dina System; KYA Technologies, Tokyo, Japan) was used for high-efficiency two-dimensional liquid chromatography experiments, with a 35 × 0.32 mm inner diameter SCX column (containing polysulfoethyl aspartamide-bonded silica particles), a 1.0 × 0.5 mm inner diameter RP trap column (containing C18 silica particles), and a 50 × 0.15 mm inner diameter RP separation column (containing C18 silica particles). The peptides were loaded onto the SCX column and washed with solvent A (0.1% vol/vol formic acid). The peptides were separated into four fractions: an unbound fraction and three eluted fractions with 50, 100, and 500 mM ammonium acetate. The peptides in each fraction were trapped on the online-connected RP trap column. Desalted peptides on the trap column were eluted from the trap column and fractionated by the RP separation column.

The peptides eluted from the RP column were analyzed by a quadrupole-time-of-flight mass spectrometer (Q-Tof Ultima; Waters-Micromass, Manchester, UK) with a heated capillary temperature of 150 C and an ESI voltage of 2.0 kV. An online nanospray emitter (New Objective, Woburn, MA) was connected to the outlet of the RP separation column for ESI. The operation protocols were followed according to the manufacturer's specifications. The Mascot program (Matrix Science, Boston, MA) was used for peptide and protein identification by searching against the Swiss-Prot database. The peptide tolerance and MS/MS tolerance were set to 2.0 and 0.8 Da, respectively.

RNA interference

RNA interference of histone H2B mRNA was performed as described (19). dsRNA was chemically synthesized by Invitrogen (stealth RNAi). Sequences of each RNA were as follows: histone H2Bl116 sense, 5′-CGGUGUACGUGUACAAGGUGCUGAA-3′; histone H2Bl169 sense, 5′-UCCAAGGCCAUGGGCAUCA-UGAACU-3′; and histone H2Bl340 sense, 5′-GGCAC-CAAGGCAGUCACCAAGUACA-3′. The cells (1×10^5) were transfected with 50 nM of each dsRNA using Lipofectamine RNAiMAX transfection reagent (Invitrogen) according to the manufacturer's protocol.

Western blotting analysis

Samples were prepared and blotting was performed as previously described (24), with minor modifications. To analyze cytosolic histone H2B, the cytosol fraction was isolated as described (25). Briefly, cells were lysed in 0.1% Nonidet P-40 lysis buffer and incubated at 4 C for 10 min. Nuclei were pelleted by centrifugation at 1000 rpm for 5 min; the cytosolic fraction was further clarified by centrifugation at 14,000 rpm for 10 min. Samples were mixed with 4× lithium dodecyl sulfate sample buffer and 10× reducing agent (Invitrogen) and incubated for 10 min at 70 C before electrophoresis. Proteins were separated on NuPAGE 4–12% Bis Tris Gel and transferred using an i-Blot Gel Transfer Device (Invitrogen). Membranes were washed with PBS with 0.1% Tween 20, incubated overnight in blocking buffer (3% bovine serum in PBS with 0.1% Tween 20), and then incubated with goat polyclonal anti β-actin (Santa Cruz Biotechnology, Santa Cruz, CA) or mouse monoclonal anti-histone H2B antibody (BioVision, Mountain View, CA) (dilution 1:1000) for 1 h at room temperature. Membranes were incubated with horseradish peroxidase (HRP)-linked antigoat IgG (GE Healthcare) or HRP-linked antimouse IgG (Millipore) (dilution 1:10000) for 1 h at room temperature. Membranes were incubated with streptavidin-peroxidase (dilution 1:10,000) for 1 h at room temperature. HRP was revealed using the Amersham ECL Plus Western Blotting Detection System (GE Healthcare).

Results

Fragments of genomic DNA are present in the cytosol of thyroid cells after cell injury

It was previously demonstrated using PCR analysis that cell injury resulted in the release of genomic DNA fragments (14). However, subcellular localization and the amount of such genomic DNA were not clear. To further evaluate the release of genomic DNA fragments into the cytosol after cell injury, FRTL-5 thyroid cells were ex-

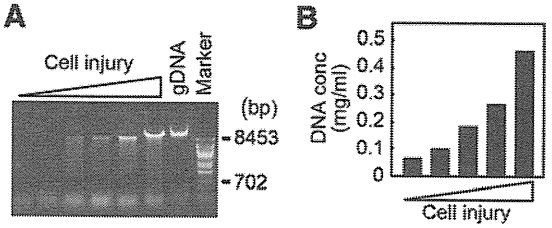

FIG. 1. Thyroid cell injury induced by electric pulse results in the release of genomic DNA into the cytosol. FRTL-5 cells were pulsed once with a Gene Pulser (Bio-Rad) at 0.5 kV and a capacitance of 0, 250, 500, 750, or 1000 μF or pulsed twice with a capacitance of 1000 μF. The cytosolic DNA fraction was isolated by sucrose density-gradient centrifugation as described in *Materials and Methods*. A, Agarose gel (0.8%) electrophoresis of the purified cytosolic DNA fraction of injured cells. Purified genomic DNA (gDNA) from intact FRTL-5 cells served as a positive control. B, Cytosolic DNA purified from each sample (1×10^7 cells) was suspended in 30 μl, and the concentration (conc) was measured using a NanoVue spectrophotometer (GE Healthcare). Typical results from at least four different experiments using different batches of cells are shown. Genomic DNA from intact FRTL-5 cells served as a positive control. DNA samples were analyzed by electrophoresis on 2% agarose gels. Genomic DNA was purified using QIAamp DNA Mini Kits (QIAGEN). DNA marker is a λ*BstP*I digest (A) (TAKARA BIO).

posed to progressively higher levels of electric pulsing. The cytosolic fraction was isolated using sucrose density-gradient centrifugation, and DNA fragments were purified by a phenol/chloroform extraction and ethanol precipitation followed by ribonuclease treatment. Agarose gel electrophoresis clearly demonstrated the appearance of DNA fragments in the cytosol in correlation with the degree of cell injury, which was observed as a smear pattern in the gel (Fig. 1A). The DNA concentration in the cytosolic preparation, as measured by an absorption spectrometer, increased significantly by cell injury (Fig. 1B), and a PCR analysis of the promoter sequence of vascular endothelial growth factor (*VEGF*) confirmed the appearance of genomic DNA in the cytosol after cell injury (Supplemental Fig. 1, published on The Endocrine Society's Journals Online web site at http://endo.endojournals.org).

Cell injury activates genes involved in both innate and acquired immune responses in thyroid cells

It has been demonstrated that stimulating cells with synthetic dsDNA or dsRNA polynucleotides activates innate and acquired immune responses in various cell types, including thyrocytes (14, 26). To further elucidate whether the sterile cell injury, *i.e.* no exogenous DNA or RNA exists, activates an innate immune response in the thyroid, we performed RT-PCR analysis of various chemokines, inflammatory cytokines, and type I IFNs after electric pulsing of FRTL-5 cells. Stimulation of cells with synthetic dsDNA or dsRNA served as controls. Cell injury clearly activated gene expression of IFN-β, TNF-α, and IL-6 as well as CC chemokine (CCL2, CCL4, and

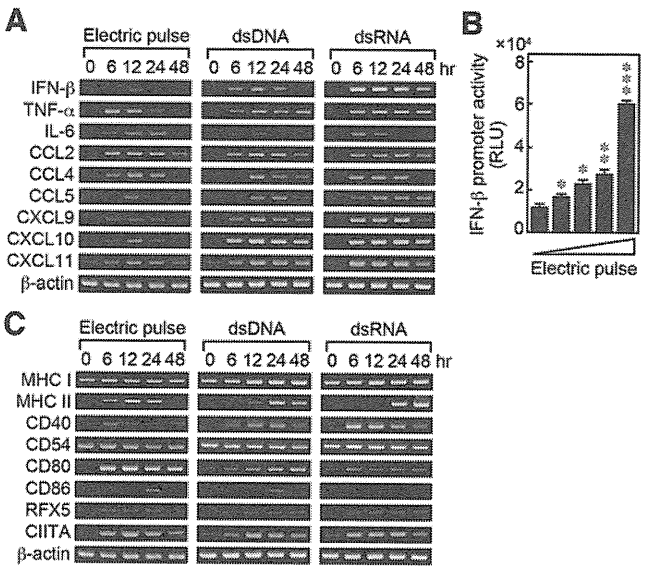

FIG. 2. Cell injury activates innate and acquired immune responses in thyroid cells. FRTL-5 cells were electrically pulsed once with 0.5 kV at a capacitance of 500 μF. Total RNA was isolated at the indicated time after stimulation, and RT-PCR was performed. FRTL-5 cells transfected with dsDNA or dsRNA in six-well plates served as controls. Typical results from at least four different experiments on different batches of cells are shown. A, RT-PCR analysis of genes related to innate immunity after cell injury. B, FRTL-5 cells were first transfected with a rat IFN-β promoter luciferase reporter gene and incubated for 24 h. Transfected cells were then electrically pulsed once with 0.5 kV at capacitances of 0, 250, 500, 750, and 1000 μF and incubated for another 24 h. Luciferase activity was expressed as means ± SD of relative light units (RLU) from four samples. *, $P \leq 1 \times 10^{-2}$; **, $P \leq 1 \times 10^{-5}$; ***, $P \leq 1 \times 10^{-8}$ compared with the control. C, RT-PCR analysis of genes related to acquired immunity after cell injury.

CCL5) and CXC chemokine (CXCL9, CXCL10, and CXCL11) families in the thyroid cells in the absence of either pathogens or immune cells (Fig. 2A). Because IFN-β is one of the most typical factors that determine innate immune activation, we examined activation of its promoter after cell injury induced by electric pulsing. Rat IFN-β promoter activity, as measured by a luciferase reporter gene assay, significantly increased in correlation with an increasing degree of cell injury induced by electric pulsing (Fig. 2B). Similar inductions of genes associated with innate immune responses were detected when cell injury was induced by removing cell culture medium for 30 min, although the induction was weaker than with electric pulsing (Supplemental Fig. 2). This evidence indicates that the observed activation of genes associated with innate immunity was general to cell injury but not specific to electric pulsing. In addition to the innate immune activation of thyroid cells, molecules necessary for antigen processing and presentation were also induced after cell injury, including MHC class I and class II and costimulatory molecules CD80 (B7.1) and CD86 (B7.2), cell adhesion molecules CD40 and CD54 [intercellular adhesion molecule-1 (ICAM-I)] that binds to CD154 (CD40 ligand) and

CD11/CD18 (β2-integlins), and essential transcriptional activators for MHC genes, *e.g.* regulatory factor X, 5 (RFX5), and class II transactivator (CIITA) (Fig. 2C).

Cell injury-induced gene expression related to innate and acquired immune responses was similar to that induced by transfecting synthetic polynucleotides, such as dsDNA and dsRNA; however, induction of IFN-β, TNF-α, CXC chemokines, and CD40 was weaker in cell injury than that observed with dsDNA/dsRNA transfection (Fig. 2, A and C). In addition, there were some notable features specific to cell injury. For example, cell injury induced MHC class II expression in 6 h, which was faster than exogenous dsDNA/dsRNA transfection, and the induction of CD80 by cell injury was much stronger than that of dsDNA/dsRNA (Fig. 2C). These differences suggest that cell injury may preferentially activate the MHC class II pathway to present antigen compared with the activation introduced by exogenous nucleic acids, *e.g.* in the event of viral infection.

dsDNA suppresses iodide uptake and RNA expression of NIS and Tg

It has been previously shown that thyroid hormone synthesis and gene expression are suppressed when immune activation was induced in the thyroid (26, 27). To investigate whether dsDNA or dsRNA affects thyroid endocrine function, we analyzed ^{125}I uptake in FRTL-5 cells after transfection of single-stranded or double-stranded nucleic acids. Both dsDNA and dsRNA significantly suppressed ^{125}I uptake of FRTL-5 cells, whereas ssDNA or ssRNA did not (Fig. 3A). mRNA levels of NIS, which is responsible for iodide uptake, were significantly suppressed by cell injury or by transfection of dsDNA or dsRNA (Fig. 3B). In addition to NIS mRNA, Tg mRNA levels were also significantly decreased by cell injury (Supplemental Fig. 3). However, expression of other thyroid-specific genes and transcription factors was not significantly affected by dsDNA (Supplemental Fig. 4). These results suggest that when thyroid cell injury occurs and fragments of genomic DNA are released, iodide uptake and its organification to Tg will be suppressed, by which the synthesis of thyroid hormone will also be reduced.

Extrachromosomal histone H2B mediates innate immune response gene expression induced by cell injury

To determine the specific molecules responsible for genomic DNA-mediated actions in FRTL-5 thyroid cells, we attempted to identify cytosolic proteins that directly bind to dsDNA. To do this, all FRTL-5 cytosolic proteins that passed through a ssDNA Sepharose column and absorbed to dsDNA Sepharose columns were purified and

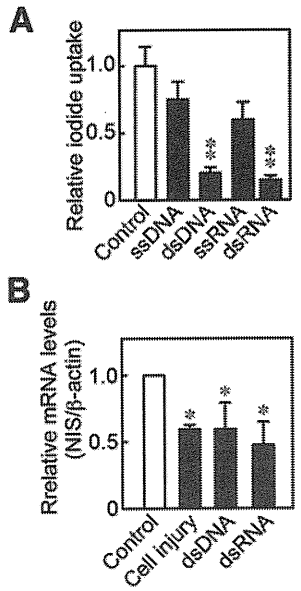

FIG. 3. Cell injury suppresses iodide uptake and NIS expression. A, FRTL-5 cells were transfected with ssDNA [poly(deoxyadenosine)], dsDNA [poly(deoxyadenosine-deoxythymidine)], ssRNA [poly(adenosine)], or dsRNA [poly(inosine-cytosine)], and radioiodine uptake was evaluated 72 h later as described in *Materials and Methods*. Data represent mean ± SD of four samples. B, Quantitative real-time PCR analysis of NIS transcripts in FRTL-5 cells 12 h after cell injury (0.5 kV, 500 μF). FRTL-5 cells transfected with dsDNA or dsRNA in six-well plates served as controls. Results are displayed relative to the original levels. Data represent mean ± SD of six samples. *, $P \leq 1\times10^{-2}$; **, $P \leq 1 \times 10^{-5}$ compared with the control.

subjected to ESI-MS/MS analysis. As a result, three kinds of histones, *i.e.* histone H1d, histone H2B, and similar to CG31613-PA (histone H3c), were identified to have significantly high Mascot (probability) scores (Table 2). We previously identified extrachromosomal histone H2B, but not H1 or H3, as a factor that senses intracellular dsDNA and mediates innate antiviral immune responses using an expression cloning strategy in HEK293T human kidney cells (19). Thus, results obtained from these two independent approaches imply that histone H2B physically associates with dsDNA in rat thyroid cells and functionally activates the IFN-β promoter in human kidney cells after dsDNA stimulation.

We next investigated whether histone H2B mediates dsDNA-induced IFN-β expression in FRTL-5 cells. To do this, small interfering RNA (siRNA) for histone H2B was used to knock down endogenous histone H2B in FRTL-5 cells. Transfection of H2B siRNA significantly suppressed the level of endogenous histone H2B protein in the cytosol (Fig. 4A). We then examined the effect of H2B knockdown on rat IFN-β promoter activation induced by dsDNA in FRTL-5 cells. As expected, transfection with histone H2B siRNA significantly suppressed IFN-β promoter activation induced by dsDNA, but not by dsRNA transfection (Fig. 4B), indicating that the function of histone H2B is specific to DNA. We then introduced cell injury after

TABLE 2. Time-of-flight mass spectrometry analysis of proteins bound to dsDNA but not to ssDNA

Mascot score	Accession no.	Name
419	gi 92378	Histone H1d - rat
401	gi 34876364	Similar to CG31613-PA (*Rattus norvegicus*)
369	gi 223096	Histone H2B
91	gi 34865887	Similar to arginine-rich, mutated in early stage tumors; EST D17914 (*R. norvegicus*)
85	gi 4504445	Heterogeneous nuclear ribonucleoprotein A1 isoform a; nuclear ribonucleoprotein particle A1 protein
83	gi 6677775	Ribosomal protein L22 (*Mus musculus*)
82	gi 2143784	Histone H2A.1, rat
78	gi 27664664	Similar to 25-kDa FK506-binding protein (*R. norvegicus*)
73	gi 27686041	Similar to histone H1 (*R. norvegicus*)
71	gi 27687007	Similar to RIKEN cDNA 1110018B13 (*R. norvegicus*)
68	gi 6681095	Cytochrome c, somatic (*M. musculus*)
68	gi 16758586	Succinate-CoA ligase, GDP-forming, α subunit (*R. norvegicus*)
67	gi 6754208	High-mobility group box 1; high mobility group protein 1 (*M. musculus*)
67	gi 67548	Trypsin (EC 3.4.21.4) II precursor, rat
64	gi 34857241	Similar to high mobility group protein 1 (HMG-1) (Amphoterin) (heparin-binding protein p30) (*R. norvegicus*)
63	gi 34875750	Similar to cell division cycle associated 3; gene rich cluster, C8 gene; trigger of mitotic entry 1
62	gi 6978563	ATPase inhibitor; ATPase inhibitor (rat mitochondrial IF1 protein) (*R. norvegicus*)
58	gi 12025520	Testis-specific histone 2a (*R. norvegicus*)
57	gi 34865253	Similar to L-lactate dehydrogenase A chain (LDH-A) (LDH muscle subunit) (LDH-M) (*R. norvegicus*)
56	gi 34852512	Similar to macroH2A2 (*R. norvegicus*)
54	gi 34878086	Similar to high mobility group 1 protein (*R. norvegicus*)
53	gi 4378711	Nucleic acid binding factor pRM10 (*R. norvegicus*)
53	gi 7446334	Telomeric and tetraplex DNA binding protein qTBP42 V, rat (fragment)
53	gi 34875658	Similar to ALY (*R. norvegicus*)

transfection of control or H2B siRNA. Histone H2B knockdown significantly suppressed cell injury-induced IFN-β promoter activation (Fig. 4C). Similarly, the IFN-β and IL-6 mRNA levels that were induced by cell injury were reduced by H2B siRNA (Fig. 4D). In addition, the NIS mRNA levels that were reduced by cell injury were ameliorated by H2B siRNA (Fig. 4E), although radioiodine uptake was difficult to measure after cell injury (data not shown). These results suggest that histone H2B actually mediates innate immune activation, which was triggered by genomic DNA released by cell injury in FRTL-5 thyroid cells.

Discussion

It was previously demonstrated that thyroid cells are capable of activating innate and acquired immune responses without interacting with immune competent cells such as macrophages and lymphocytes (14, 28, 29). In such cases, various pathogen-associated molecular patterns, such as lipopolysaccharide, dsDNA, and dsRNA, were thought to function as exogenous adjuvants to activate immune response (14, 26, 30). However, clinical observations have suggested that immune responses were similarly activated without evidence of infection (31–34). Potential endogenous adjuvants in the thyroid, which may be released in the context of tissue damage that can activate innate immune responses, are not well understood. In this study, we have shown that thyroid cell injury induced under sterile conditions activates genes involved in both innate and acquired immune responses and suppresses thyroid function. We then determined that fragments of genomic DNA released into the cytosol of injured cells, which is recognized by extrachromosomal histone H2B, are the factors responsible for these effects.

Genomic DNA is normally sequestered in the nucleus but can be released when cells undergo necrosis or apoptosis. It has been shown that dsDNA derived from host cells or pathogens or those chemically synthesized can similarly activate both immune cells (macrophages or dendritic cells) and nonimmune cells (fibroblasts, myocytes, or thyroid cells) when introduced into the cytosol (12, 14, 35). The action is not dependent on DNA sequence but does require a double-stranded helical structure (14), especially right-handed B-form DNA (35). dsDNA activates a set of genes, including those encoding MHC, costimulatory molecules, transporter associated with antigen processing (TAP1), and immunoproteasome subunits large multifunctional protease 2, as well as the signal transducer and activator of transcription 1 (STAT1), IRFs, and protein kinase R (PKR) (12, 14).

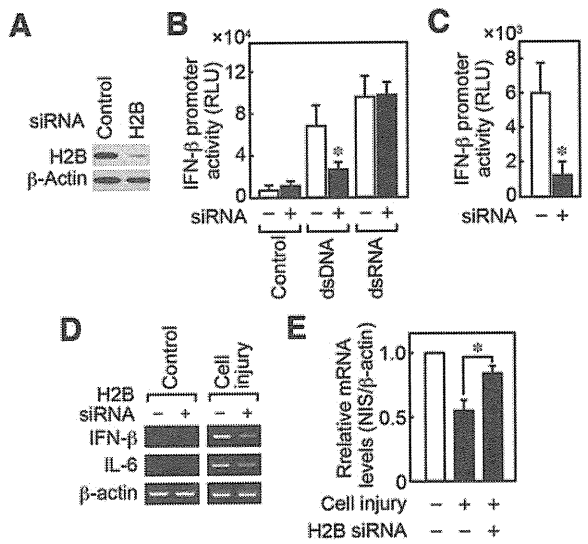

FIG. 4. Histone H2B mediates cell injury-induced IFN-β expression in rat thyroid FRTL-5 cells. A, Effect of siRNA targeting histone H2B to reduce cytoplasmic H2B protein levels was evaluated by immunoblotting analysis using anti-H2B or antiactin antibodies 48 h after transfection. B, Effect of histone H2B siRNA was examined for rat IFN-β promoter activity in cells stimulated with dsDNA or dsRNA. Data represent mean ± SD of four samples. C, Effect of histone H2B siRNA on rat IFN-β promoter activity in cells injured by electric pulsing with 0.5 kV, 500 μF. Luciferase assay was performed 12 h after cell injury. Data represent mean ± SD of four samples. D, RT-PCR analysis for IFN-β and IL-6 expression induced by cell injury for 12 h with or without histone H2B siRNA treatment. E, Quantitative real-time PCR analysis of NIS transcripts in FRTL-5 cells 48 h after cell injury (0.5 kV, 500 μF) with or without histone H2B siRNA treatment. Data represent mean ± SD of six samples. *, $P \leq 1 \times 10^{-2}$ compared with the control.

Our data indicate that genomic DNA fragments released from injured or apoptotic cells act as a danger signal to alert the host immune system. This phenomenon is corroborated by an observation of liver macrophages in DNase II-deficient mice that underwent lethal anemia in embryos (36). A large amount of IFN-β was produced by these macrophages, associated with an accumulation of undigested DNA derived from phagocytosed nuclei of erythroblasts. Conditional DNase II-deficient mice that have survived lethal embryonic anemia develop rheumatoid arthritis-like symptoms and exhibited hyperproduction of proinflammatory cytokines, such as TNF-α, IL-1β, IL-6, and IL-10 as well as type I IFNs (13). In addition, DNase I-deficient mice showed classical symptoms of systemic lupus erythematosus, including production of antinuclear antibodies against genomic DNA and nucleosomes (37). DNase III-deficient mice developed inflammatory myocarditis (38). The fact that fragments of dsDNA have an adjuvant effect *in vivo* and induce MHC expression in various cell types (12, 14) may support the development of these phenotypes in the mice where genomic DNA cannot be properly digested and remained excessively within cytosol.

Recently, several proteins have been reported as candidates that recognize cytosolic dsDNA and induce IFN-β expression, such as ZBP1 (15), RIG-I (16, 17), and extrachromosomal histone H2B (19). Although these molecules seem to be involved in the recognition of cytosolic dsDNA, it is plausible to suppose that the functions are different among species and cell types. In this study, we have comprehensively determined the cytosolic molecules that physically bind to dsDNA using mass spectrometry. We have successfully identified histone H2B, which has also been reported to be a mediator of dsDNA action by interacting with IFN-β promoter stimulator-1, an essential adaptor molecule, in human cells (19), as a responsible molecule that physically binds to dsDNA and functionally mediates the activation of inflammatory genes in thyroid cells.

It is well known that histone H2B is usually assembled in the nucleosome with genomic DNA as a core histone. However, it is also known that histone exchange and deposition often take place in living cells and that histones have functions other than nucleosome assembly. Thus, an exchange of histone H2A/H2B and nucleosome sliding mediated by nucleosome assembly protein 1 increases chromatin fluidity (39). It was demonstrated that histone H2A.X is phosphorylated by responding to dsDNA breaks (40). Also, histone H1.2 was shown to be a cytochrome c-releasing factor that appears in the cytoplasm after exposure to x-ray irradiation (41). This evidence supports the idea that histone H2B can be released from the nucleosome and recognizes extrachromosomal genomic DNA fragments in the cytosol, which activates signal transduction pathways (19). Further investigation of the function of extrachromosomal histone H2B will help in understanding the biological relevance of DNA-sensing mechanisms in the cytosol.

Aberrant MHC class II expression has been reported in various autoimmune target tissues, including thyroid follicular cells in Graves' disease patients (42). Our results suggest that cell injury activates the intrinsic MHC class II pathway in the thyroid cells, which in turn may contribute to the presentation of thyroid autoantigens that may trigger autoimmune responses. In an animal model for Graves' disease, it was demonstrated that the TSH receptor-stimulating antibody that causes Graves' disease was produced only when MHC class II and TSH receptor were coexpressed in the same cell (43). It was also shown that double-transgenic mice expressing costimulatory B7 and TNF-α in the pancreatic islet cells developed autoimmune diabetes (44). Furthermore, MHC class II-producing hepatocytes with costimulatory B7 molecules on their surface could present antigen and activate CD4 T cells (45). We have demonstrated that genomic DNA fragments released by cell injury are the factors responsible for the activation of intrinsic immune function of the thyroid.

Etiology of autoimmune diseases largely remains a mystery. Infections and injuries often precede autoimmune attack, but how those events make the immune system attack its own tissue is still unclear. Increasing evidence supports the ability of infection or cell damage to activate intracellular signaling cascades and to increase MHC gene expression in nonimmune cells (2, 10, 46). Our previous and present findings uncover a novel mechanism of misplaced DNA in double-stranded form (dsDNA) in the cytosol to lead cells to present self-antigen and to rally the immune system (12, 14, 35). Our results support the hypothesis that factors released by dying host cells facilitates the induction of immunity against foreign and/or self-antigens (10).

Based on the present and previous observations (12, 14, 19, 35), we propose the following consequences. Thyroid cell damage prompts the release of genomic DNA fragments that will leak into or be endocytosed by neighboring cells. Extrachromosomal histone H2B binds to exposed dsDNA in the cytosol through COOH-terminal importin 9-related adaptor organizing histone H2B and IFN-β promoter stimulator-1 (CIAO) (19) and then signals such as IRF and nuclear factor-κB are activated (47). These result in the production of type I IFNs, proinflammatory cytokines, and chemokines, which not only recruit and activate immune cells but also stimulate thyroid follicular cells in an autocrine and/or paracrine manner to induce MHC expression. We have previously shown that dsDNA activates all the essential genes necessary for antigen processing and presentation and induces cell surface MHC expression (12, 14, 35). When these events take place in addition to the autoimmune-prone genetic factors such as MHC haplotype and other environmental factors (1), a vicious circle of autoimmune reaction may be initiated. Ligation of Fas and Fas ligand results in apoptotic suicide or fratricide of thyrocytes (9).

It is noteworthy that cell injury induced MHC class II expression faster than exogenous dsDNA/dsRNA stimulation and induced much stronger expression of costimulatory molecules. Although proximal and distal promoters are required to activate MHC class II expression (48), such a fast induction may suggest the existence of other mechanisms that are responsible for the MHC class II transcription, such as epigenetic activation (49). Whether or not histone H2B plays a role in this regard is under investigation in our laboratory.

Cell injury selectively suppressed the mRNA expression of NIS and Tg among thyroid-specific genes responsible for proper endocrine function. This effect may be explained by the secreted cytokines as reported (8, 26, 28, 29), although other possible mechanisms other than that involving genomic DNA may also be involved. Decreases in iodide uptake induced by thyroid cell injury will result in a decrease of hormone synthesis and eventually thyroid dysfunction. Thus, this mechanism may contribute to the development of hypothyroidism seen in cases of thyroid inflammation. Further studies to evaluate the effect of cell injury in thyroid tissues *in vivo*, *e.g.* using laser irradiation (50) or *in vivo* electroporation (51), will be needed to confirm our *in vitro* results. Also, similar studies using other cells will also be important because cell injury could prompt the release of genomic DNA fragments in any cell types.

In summary, we have demonstrated that thyroid cell injury results in the release of genomic DNA fragments into the cytosol. Such dsDNA is recognized by extrachromosomal histone H2B to activate genes involved in both innate and acquired immune responses. The endocrine function of the thyroid is suppressed at least in part by the same mechanism. These findings may be associated with the development of autoimmune thyroid disorders and also thyroid dysfunctions that may occur after thyroid cell injury due to ischemic, traumatic, or other destructive changes in the absence of possible infection.

Acknowledgments

Address all correspondence and requests for reprints to: Dr. Koichi Suzuki. Laboratory of Molecular Diagnostics, Department of Mycobacteriology, Leprosy Research Center, National Institute of Infectious Diseases, 4-2-1 Aoba-cho, Higashimurayama, Tokyo 189-0002, Japan. E-mail: koichis@nih.go.jp.

This work was supported by a Grant-in-Aid for Scientific Research from the Japan Society for the Promotion of Science (15390296 and 21591187 to K.S.).

Disclosure Summary: The authors have nothing to disclose.

References

1. **Jacobson EM, Tomer Y** 2007 The genetic basis of thyroid autoimmunity. Thyroid 17:949–961
2. **Mackay IR, Leskovsek NV, Rose NR** 2008 Cell damage and autoimmunity: a critical appraisal. J Autoimmun 30:5–11
3. **Luo G, Seetharamaiah GS, Niesel DW, Zhang H, Peterson JW, Prabhakar BS, Klimpel GR** 1994 Purification and characterization of *Yersinia enterocolitica* envelope proteins which induce antibodies that react with human thyrotropin receptor. J Immunol 152:2555–2561
4. **Horwitz MS, Bradley LM, Harbertson J, Krahl T, Lee J, Sarvetnick N** 1998 Diabetes induced by Coxsackie virus: initiation by bystander damage and not molecular mimicry. Nat Med 4:781–785
5. **Desailloud R, Hober D** 2009 Viruses and thyroiditis: an update. Virol J 6:5
6. **Lazarus JH, Parkes AB, Premawardhana LD** 2002 Postpartum thyroiditis. Autoimmunity 35:169–173
7. **Nishihara E, Ohye H, Amino N, Takata K, Arishima T, Kudo T, Ito M, Kubota S, Fukata S, Miyauchi A** 2008 Clinical characteristics of

852 patients with subacute thyroiditis before treatment. Intern Med 47:725–729
8. Yamazaki K, Tanigawa K, Suzuki K, Yamada E, Yamada T, Takano K, Obara T, Sato K 2010 Iodide-induced chemokines and genes related to immunological function in cultured human thyroid follicles in the presence of thyrotropin. Thyroid 20:67–76
9. Giordano C, Stassi G, De Maria R, Todaro M, Richiusa P, Papoff G, Ruberti G, Bagnasco M, Testi R, Galluzzo A 1997 Potential involvement of Fas and its ligand in the pathogenesis of Hashimoto's thyroiditis. Science 275:960–963
10. Kono H, Rock KL 2008 How dying cells alert the immune system to danger. Nat Rev Immunol 8:279–289
11. Shi Y, Evans JE, Rock KL 2003 Molecular identification of a danger signal that alerts the immune system to dying cells. Nature 425: 516–521
12. Ishii KJ, Suzuki K, Coban C, Takeshita F, Itoh Y, Matoba H, Kohn LD, Klinman DM 2001 Genomic DNA released by dying cells induces the maturation of APCs. J Immunol 167:2602–2607
13. Kawane K, Ohtani M, Miwa K, Kizawa T, Kanbara Y, Yoshioka Y, Yoshikawa H, Nagata S 2006 Chronic polyarthritis caused by mammalian DNA that escapes from degradation in macrophages. Nature 443:998–1002
14. Suzuki K, Mori A, Ishii KJ, Saito J, Singer DS, Klinman DM, Krause PR, Kohn LD 1999 Activation of target-tissue immune-recognition molecules by double-stranded polynucleotides. Proc Natl Acad Sci USA 96:2285–2290
15. Takaoka A, Wang Z, Choi MK, Yanai H, Negishi H, Ban T, Lu Y, Miyagishi M, Kodama T, Honda K, Ohba Y, Taniguchi T 2007 DAI (DLM-1/ZBP1) is a cytosolic DNA sensor and an activator of innate immune response. Nature 448:501–505
16. Choi MK, Wang Z, Ban T, Yanai H, Lu Y, Koshiba R, Nakaima Y, Hangai S, Savitsky D, Nakasato M, Negishi H, Takeuchi O, Honda K, Akira S, Tamura T, Taniguchi T 2009 A selective contribution of the RIG-I-like receptor pathway to type I interferon responses activated by cytosolic DNA. Proc Natl Acad Sci USA 106:17870–17875
17. Chiu YH, Macmillan JB, Chen ZJ 2009 RNA polymerase III detects cytosolic DNA and induces type I interferons through the RIG-I pathway. Cell 138:576–591
18. Hornung V, Ablasser A, Charrel-Dennis M, Bauernfeind F, Horvath G, Caffrey DR, Latz E, Fitzgerald KA 2009 AIM2 recognizes cytosolic dsDNA and forms a caspase-1-activating inflammasome with ASC. Nature 458:514–518
19. Kobiyama K, Takeshita F, Jounai N, Sakaue-Sawano A, Miyawaki A, Ishii KJ, Kawai T, Sasaki S, Hirano H, Ishii N, Okuda K, Suzuki K 2010 Extrachromosomal histone H2B mediates innate antiviral immune responses induced by intracellular double-stranded DNA. J Virol 84:822–832
20. Ishii KJ, Kawagoe T, Koyama S, Matsui K, Kumar H, Kawai T, Uematsu S, Takeuchi O, Takeshita F, Coban C, Akira S 2008 TANK-binding kinase-1 delineates innate and adaptive immune responses to DNA vaccines. Nature 451:725–729
21. Ablasser A, Bauernfeind F, Hartmann G, Latz E, Fitzgerald KA, Hornung V 2009 RIG-I-dependent sensing of poly(dA:dT) through the induction of an RNA polymerase III-transcribed RNA intermediate. Nat Immunol 10:1065–1072
22. Suzuki K, Yanagi M, Mori-Aoki A, Moriyama E, Ishii KJ, Kohn LD 2002 Transfection of single-stranded hepatitis A virus RNA activates MHC class I pathway. Clin Exp Immunol 127:234–242
23. Suzuki K, Kohn LD 2006 Differential regulation of apical and basal iodide transporters in the thyroid by thyroglobulin. J Endocrinol 189:247–255
24. Suzuki K, Mori A, Saito J, Moriyama E, Ullianich L, Kohn LD 1999 Follicular thyroglobulin suppresses iodide uptake by suppressing expression of the sodium/iodide symporter gene. Endocrinology 140:5422–5430
25. Bauler LD, Duckett CS, O'Riordan MX 2008 XIAP regulates cytosol-specific innate immunity to Listeria infection. PLoS Pathog 4:e1000142
26. Yamazaki K, Suzuki K, Yamada E, Yamada T, Takeshita F, Matsumoto M, Mitsuhashi T, Obara T, Takano K, Sato K 2007 Suppression of iodide uptake and thyroid hormone synthesis with stimulation of the type I interferon system by double-stranded ribonucleic acid in cultured human thyroid follicles. Endocrinology 148:3226–3235
27. Mori-Aoki A, Pietrarelli M, Nakazato M, Caturegli P, Kohn LD, Suzuki K 2000 Class II transactivator suppresses transcription of thyroid-specific genes. Biochem Biophys Res Commun 278:58–62
28. Sato K, Satoh T, Shizume K, Ozawa M, Han DC, Imamura H, Tsushima T, Demura H, Kanaji Y, Ito Y, Obara T, Fujimoto Y, Kanaji Y 1990 Inhibition of ^{125}I organification and thyroid hormone release by interleukin-1, tumor necrosis factor-α, and interferon-γ in human thyrocytes in suspension culture. J Clin Endocrinol Metab 70:1735–1743
29. Yamazaki K, Yamada E, Kanaji Y, Shizume K, Wang DS, Maruo N, Obara T, Sato K 1996 Interleukin-6 (IL-6) inhibits thyroid function in the presence of soluble IL-6 receptor in cultured human thyroid follicles. Endocrinology 137:4857–4863
30. Nicola JP, Vélez ML, Lucero AM, Fozzatti L, Pellizas CG, Masini-Repiso AM 2009 Functional toll-like receptor 4 conferring lipopolysaccharide responsiveness is expressed in thyroid cells. Endocrinology 150:500–508
31. Lassen S, Lech M, Römmele C, Mittruecker HW, Mak TW, Anders HJ 2010 Ischemia reperfusion induces IFN regulatory factor 4 in renal dendritic cells, which suppresses postischemic inflammation and prevents acute renal failure. J Immunol 185:1976–1983
32. Paterson HM, Murphy TJ, Purcell EJ, Shelley O, Kriynovich SJ, Lien E, Mannick JA, Lederer JA 2003 Injury primes the innate immune system for enhanced Toll-like receptor reactivity. J Immunol 171: 1473–1483
33. Pickup JC, Mattock MB, Chusney GD, Burt D 1997 NIDDM as a disease of the innate immune system: association of acute-phase reactants and interleukin-6 with metabolic syndrome X. Diabetologia 40:1286–1292
34. Turina M, Fry DE, Polk Jr HC 2005 Acute hyperglycemia and the innate immune system: clinical, cellular, and molecular aspects. Crit Care Med 33:1624–1633
35. Ishii KJ, Coban C, Kato H, Takahashi K, Torii Y, Takeshita F, Ludwig H, Sutter G, Suzuki K, Hemmi H, Sato S, Yamamoto M, Uematsu S, Kawai T, Takeuchi O, Akira S 2006 A Toll-like receptor-independent antiviral response induced by double-stranded B-form DNA. Nat Immunol 7:40–48
36. Yoshida H, Okabe Y, Kawane K, Fukuyama H, Nagata S 2005 Lethal anemia caused by interferon-β produced in mouse embryos carrying undigested DNA. Nat Immunol 6:49–56
37. Napirei M, Karsunky H, Zevnik B, Stephan H, Mannherz HG, Möröy T 2000 Features of systemic lupus erythematosus in Dnase1-deficient mice. Nat Genet 25:177–181
38. Morita M, Stamp G, Robins P, Dulic A, Rosewell I, Hrivnak G, Daly G, Lindahl T, Barnes DE 2004 Gene-targeted mice lacking the Trex1 (DNase III) 3′–>5′ DNA exonuclease develop inflammatory myocarditis. Mol Cell Biol 24:6719–6727
39. Kimura H 2005 Histone dynamics in living cells revealed by photobleaching. DNA Repair (Amst) 4:939–950
40. Redon C, Pilch D, Rogakou E, Sedelnikova O, Newrock K, Bonner W 2002 Histone H2A variants H2AX and H2AZ. Curr Opin Genet Dev 12:162–169
41. Konishi A, Shimizu S, Hirota J, Takao T, Fan Y, Matsuoka Y, Zhang L, Yoneda Y, Fujii Y, Skoultchi AI, Tsujimoto Y 2003 Involvement of histone H1.2 in apoptosis induced by DNA double-strand breaks. Cell 114:673–688
42. Bottazzo GF, Pujol-Borrell R, Hanafusa T, Feldmann M 1983 Role of aberrant HLA-DR expression and antigen presentation in induction of endocrine autoimmunity. Lancet 2:1115–1119
43. Shimojo N, Kohno Y, Yamaguchi K, Kikuoka S, Hoshioka A, Niimi

H, Hirai A, Tamura Y, Saito Y, Kohn LD, Tahara K 1996 Induction of Graves-like disease in mice by immunization with fibroblasts transfected with the thyrotropin receptor and a class II molecule. Proc Natl Acad Sci USA 93:11074–11079

44. **Guerder S, Picarella DE, Linsley PS, Flavell RA** 1994 Costimulator B7-1 confers antigen-presenting-cell function to parenchymal tissue and in conjunction with tumor necrosis factor α leads to autoimmunity in transgenic mice. Proc Natl Acad Sci USA 91:5138–5142
45. **Herkel J, Jagemann B, Wiegard C, Lazaro JF, Lueth S, Kanzler S, Blessing M, Schmitt E, Lohse AW** 2003 MHC class II-expressing hepatocytes function as antigen-presenting cells and activate specific CD4 T lymphocyutes. Hepatology 37:1079–1085
46. **Moffett CW, Paden CM** 1994 Microglia in the rat neurohypophysis increase expression of class I major histocompatibility antigens following central nervous system injury. J Neuroimmunol 50:139–151
47. **Kawai T, Akira S** 2006 Innate immune recognition of viral infection. Nat Immunol 7:131–137
48. **Masternak K, Peyraud N, Krawczyk M, Barras E, Reith W** 2003 Chromatin remodeling and extragenic transcription at the MHC class II locus control region. Nat Immunol 4:132–137
49. **Gialitakis M, Kretsovali A, Spilianakis C, Kravariti L, Mages J, Hoffmann R, Hatzopoulos AK, Papamatheakis J** 2006 Coordinated changes of histone modifications and HDAC mobilization regulate the induction of MHC class II genes by Trichostatin A. Nucleic Acids Res 34:765–772
50. **Höfling DB, Chavantes MC, Juliano AG, Cerri GG, Romão R, Yoshimura EM, Chammas MC** 2010 Low-level laser therapy in chronic autoimmune thyroiditis: a pilot study. Lasers Surg Med 42:589–596
51. **Sasaki S, Smith JM, Takase K, Okuda K, Ishii N, Takeshita F** 2006 Activator protein 1-mediated transcriptional regulation strategy sustains long-term expression of a xenogeneic gene product in vivo: an implication for gene therapy targeting congenital protein deficiencies. Int J Mol Med 18:289–297

JOURNAL OF PROTEOMICS 75 (2012) 1718–1731

Available online at www.sciencedirect.com

SciVerse ScienceDirect

www.elsevier.com/locate/jprot

Effects of growth hormone on the salmon pituitary proteome

Yoichi Kurata[a], Yayoi Kimura[a], Yuko Yamanaka[a], Akiyo Ishikawa[a], Hiroyuki Okamoto[b], Tetsuji Masaoka[b], Hiroyuki Nagoya[b], Kazuo Araki[b], Shunsuke Moriyama[c], Hisashi Hirano[a,*], Tsukasa Mori[d,**]

[a]Graduate School of Nanobioscience, Yokohama City University, Suehiro 1-7-29, Tsurumi, Yokohama 230-0045, Japan
[b]Cell Engineering Section, Division of Genetics, National Research Institute of Aquaculture, Hiruta 224-1, Tamaki, Watarai, Mie 519-0423, Japan
[c]School of Marine Biosciences, Kitasato University, Kitasato 1-15-1, Sagamihara, Kanagawa 252-0373, Japan
[d]Department of Nihon University College of Bioresource Sciences, Kameino 1866, Fujisawa 252-0880, Japan

ARTICLE INFO

Article history:
Received 3 October 2011
Accepted 4 December 2011
Available online 20 December 2011

Keywords:
GH
Endocrine
Pituitary
Salmon
Proteome

ABSTRACT

Growth hormone 1 (GH1), a pituitary hormone, plays a key role in the regulation of growth. Both excess GH1 treatment and overexpression of a GH1 transgene promote growth of salmon, but these animals exhibit physiological abnormalities in viability, fertility and metabolism, which might be related to pituitary function. However, the molecular dynamics induced in the pituitary by excess GH1 remain unknown. In this study, we performed iTRAQ proteome analysis of the amago salmon pituitary, with and without excess GH1 treatment, and found that the expression levels of proteins related to endocrine systems, metabolism, cell growth and proliferation were altered in the GH1-treated pituitary. Specifically, pituitary hormone prolactin (2.29 fold), and somatolactin α (0.14 fold) changed significantly. This result was confirmed by proteome and transcriptome analyses of pituitary from the GH1-transgenic (GH1-Tg) amago salmon. The dynamics of protein and gene expression in the pituitary of GH1-Tg amago salmon were similar to those of pituitary treated with excess GH1. Our findings suggest that not only excess GH1 hormone, but also the quantitative changes in other pituitary hormones, might be essential for the abnormal growth of amago salmon. These data will be useful in future attempts to increase the productivity of fish farming.

1. Introduction

Pituitary, an endocrine organ, synthesizes and secretes various peptide hormones including growth hormone (GH), prolactin (PRL), somatolactin (SL), thyroid-stimulating hormone (TSH), luteinizing hormone (LH) and follicle-stimulating hormone (FSH) [1]. The pituitary also produces adrenocorticotropic hormone (ACTH), melanocyte-stimulating hormone (MSH) and β-endorphin, all of which are generated by proteolytic cleavage of a common pro-hormone, proopiomelanocortin (POMC) [1].

Each pituitary hormone is released into the bloodstream and each acts on different target organs in order to strictly regulate a variety of biological functions [2] such as the stress response [3], appetite [4,5] sexual maturation [2,6], thereby helping to maintain physiological homeostasis, growth and reproduction. Simultaneously, the synthesis and secretion of these hormones are controlled by hormonal feedback regulation systems [7].

Among the pituitary hormones, GH is classified into two divergent paralogs in fish, *GH1* and *GH2* [8]. GH1 has been well studied [7,10–12], though the function of GH2 is not well understood

* *Corresponding author.* Tel.: +81 45 508 7439; fax: +81 45 508 7667.
** *Corresponding author.* Tel./fax: +81 466 84 3682.
E-mail addresses: hirano@yokohama-cu.ac.jp (H. Hirano), mori.tsukasa@nihon-u.ac.jp (T. Mori).

1874-3919/$ – see front matter © 2011 Elsevier B.V. All rights reserved.
doi:10.1016/j.jprot.2011.12.009

[9]. In target tissues, GH1 binds to the GH receptor (GHR), and also acts indirectly through locally GH1-induced IGF-I production [7,10–13], in order to promote proliferation and differentiation of muscle, bone and cartilage cells. Manipulation of GH1 levels would therefore be an important potential means of increasing the productivity of fish farming [14,15].

GH1-treated/GH1 transgenic fish frequently exhibit physiological abnormalities, such as reductions of viability [16], fertility [17], and alteration of metabolism [18,19]. However, the details of the molecular dynamics in GH1-treated fish remain unknown.

In this study, we investigated the effects of excess GH1 on amago salmon pituitary. In order to identify pituitary proteins induced by excess GH1 treatment, we performed comprehensive and quantitative iTRAQ proteome analysis of the pituitary under cultured condition with and without excess GH1. In these experiments, we identified both up-regulated and down-regulated pituitary proteins involved in regulation of endocrine systems, metabolism, cell growth and proliferation. We used bioinformatic analysis to predict the phenotypes that would be affected by alterations in levels of these proteins. Furthermore, in order to confirm the relationship between excess GH1 and the regulation of proteins, we generated GH1-transgenic (GH1-Tg) amago salmon, characterized GH1-Tg phenotypes, and performed comparative quantitative proteome and transcriptome analyses of pituitary from GH1-Tg and non-transgenic (non-Tg) amago salmon. We observed that the dynamics of protein and gene expression in the pituitary of GH1-Tg amago salmon were similar to those observed in pituitary treated with excess GH1.

Based on these results, we hypothesized that not only excess GH1 hormone, but also quantitative changes in levels of the other pituitary hormones, might be important determinants of the abnormal growth of amago salmon. These findings will be important in efforts to increase the productivity of fish farming.

2. Materials and methods

2.1. *Pituitary culture for proteome analysis*

Amago salmon (*Oncorhynchus masou ishikawae*) were grown in circular tanks at 15 °C under a natural light cycle at the Fisheries Research Agency of the National Research Institute of Aquaculture in Japan. For proteome analysis, pituitaries were removed from 20 ice-anesthetized sexually immature amago salmon and immersed in ice-cold RPMI medium containing 20 mM Hepes, 9 mM sodium bicarbonate, 100 U/ml penicillin, 100 U/ml streptomycin, and 0.25 mg/ml fungizone. Next, pituitaries were incubated separately for 4 days at 12 °C in medium for organ culture [RPMI medium supplemented with 10% fetal calf serum, 100 U/ml penicillin, 100 U/ml streptomycin, and 0.25 mg/ml fungizone] with or without excess purified bovine GH1 (12.5 μg/ml, >95% pure) in order to examine the effect of excess GH1 on pituitary proteins dynamics. The method was followed by the previous report for organ culture condition of pituitary [20]. It is well known that mammalian GH1, including bovine, can bind to the fish GH1 receptor, and stimulate the growth of salmon. After culture, each pituitary was washed twice with cold PBS and homogenized in 1 ml lysis buffer [7 M urea, 2 M thiourea, 4% (w/v) CHAPS, 2% (w/v) DTT, 0.05% (w/v) SDS, and protease inhibitor cocktail] using a Polytron homogenizer (Kinematica, Bohemia, NY, USA) on ice, followed by centrifugation at 18,850 g for 30 min at 4 °C. The cleared supernatant was re-centrifuged at 69,600 g for 60 min at 4 °C. The final supernatant was stored at −80 °C until further use.

2.2. *Proteome analysis using iTRAQ reagents*

For iTRAQ labeling, the protein sample buffer was exchanged with 10 mM triethylammonium bicarbonate buffer, pH 8.5 (Sigma-Aldrich, St. Louis, MO, USA) using Microsep™ 3 k Centrifugal Devices (Pall, Port Washington, NY, USA). The protein concentration of samples was determined with a PROTEIN ASSAY kit (Bio-Rad Laboratories, Rockville, MD, USA), using bovine serum albumin as a protein standard. After cysteine blocking with methyl methanethiol sulfonate (MMTS), 32 μg of each protein sample was digested with trypsin. The resultant peptides were labeled with iTRAQ regents (AB-Sciex, Foster City, CA, USA) (Supplementary Fig. 1). After iTRAQ labeling, the samples were combined in a 1:1 ratio (v/v). Half of the combined mixtures of iTRAQ-labeled peptides were subsequently fractionated by a 2D-liquid chromatography system equipped with a strong cation exchange (SCX) column [HiQ Sil SCX, 0.5 mm inside diameter (id)×35 mm, KYA Tech, Tokyo, Japan] in the first-dimension separation, and a reverse-phase (RP) trap column (HiQ Sil C18-3, 0.8 mm id×3 mm, KYA Tech) in the second-dimension separation. The details of fractionation are provided in Supplementary Fig. 1. The fractionated peptides were automatically mixed with the MALDI matrix solution (4 mg/ml α-cyano-4-hydroxycinnamic acid dissolved in 80 μg/ml dibasic ammonium citrate containing 0.1% TFA and 70% acetonitrile), and directly spotted onto four ABI 4800 MALDI plates using a MALDI plate spotter (DiNa Direct Nano-flow LC system; KYA Tech). MS and MS/MS analyses of iTRAQ-labeled peptides were carried out on a MALDI-TOF/TOF mass spectrometer (4800 Proteomics Analyzer; AB-Sciex) in positive ion reflection mode using the 4000 Series Explorer Software (Ver. 3.5; AB-Sciex). The instrument laser power was set to 2800 for MS and 3600 for MS/MS acquisition. Typically, 1000 laser shots were accumulated per well, and MS spectra were acquired from 800 to 4000 Da with a minimum S/N filter of 50 for precursor ion selection. MS/MS analyses were performed for the 10 most abundant precursor ions per well, with an accumulation of 2000 shots for each spectrum. In order to look for less abundant proteins, re-interrogation of the target plates was carried out to acquire the 10 next-most intense peaks (if any were above the S/N threshold of 25). The series of total MS and MS/MS spectrum measurements was performed in duplicate, and these results were combined for data analysis.

MS and MS/MS data were analyzed using the ProteinPilot software ver 3.0 (AB-Sciex), which employs the Paragon algorithm for protein identification and relative quantitation [21]. The database (147,591 entries) consisted of amino acid sequences of fish proteins, retrieved from a subset of the NCBI non-redundant (nr) protein database (accessed April 14 2009) used for this search. The search parameters included iTRAQ labeling at N-terminus and lysine, cysteine modification by MMTS, methionine oxidation, and biological modifications predefined in the software. Other